Optical and microstructural properties of pure and Ru doped SnO$_2$ semiconducting thin films

O. MERMER[*], H. SOZBILEN
Ege University, Department of Electrical and Electronic Engineering, Bornova, 35100 Izmir TURKEY

Pure and ruthenium (Ru) doped nanostructure SnO$_2$ (Ru-SnO$_2$) semiconductor films were prepared by sol-gel technique on glass substrates. The effect of Ru incorporation on microstructure and optical properties of SnO$_2$ films was investigated. Crystalline structure, orientations, morphological, optical properties of the films were investigated by using XRD, SEM, AFM, VEECO profilometer, and UV spectrophotometer, respectively. The optical band gap, refractive index, extinction coefficient and dielectric constants were calculated by using transmittance and reflectance spectrum of the films. The obtained structural data indicated that all the films possess polycrystalline structure with tetragonal rutile SnO$_2$ and Ru incorporation conducts to significant changes in the microstructure of the SnO$_2$ films. In addition to these, the highest average optical transmittance value was obtained in the visible region for pure SnO$_2$ film. It was found that optical band gap of film was decreased with the increase in Ru doping, and absorption edge shifted to higher wavelengths with incorporation of Ru.

1. Introduction

Transparent conducting oxides have certain advantages when compared to other types of semiconductors, such as low cost, simple construction, small size and ease of placing the sensor in the operating environment. Therefore they are the popular and useful sensing materials for making inexpensive gas sensing devices [1]. Tin (IV) oxide is a semiconductor with a wide direct forbidden band gap of 3.6 eV and it is amenable to n-type doping. It has attracted much attention for applications involving transparent electrodes, solar cells [6] and gas sensors since it is non toxic, inexpensive, and highly abundant [3,4]. Sensors in the form of thin or thick films are very attractive because they have shown distinct advantages, such as small size, simple construction, low cost and little weight [2]. SnO$_2$ films are prepared by various fabrication techniques such as chemical vapor deposition [1], spray pyrolysis [2, 3], thermal evaporation [4], magnetron sputtering [5], and sol–gel method [6,7]. Of these methods, the sol-gel process has recently attracted considerable attention inasmuch as it is proving to be an economical and energy saving method to deposit high quality films on large areas [8].

Appropriate doping can affect the physical, optical and electrical properties of SnO$_2$ films. Even though extensive studies about the effects of dopants were carried out, there are still remaining unclear points for dopants and fabrication methods. In the literature various scientists have previously demonstrated that different elements such as Mg [9], Mn [10], Cu [11], F [12], Cs [13], Sb [14], In [15] were doped into SnO2 to modify the electrical, optical and structural properties of thin films.

The present study mainly aims to investigate the Ru incorporation on the structural and optical properties of SnO$_2$ films deposited by sol-gel method. To the best of our knowledge, this is the first report on the understanding of Ru incorporation on semiconducting SnO$_2$ films.

2. Experimental details

Undoped and Ru doped SnO$_2$ films were deposited on glass substrate by sol-gel technique. Tin (II) chloride dihydrate (Aldrich) precursor was used as starting material. The dopant source of ruthenium came from ruthenium (III) chloride (Aldrich). These salts were first dissolved in methanol at room temperature. Small amounts of glacial acetic acid were added to all solutions as chealating agent to form more than one bond to a metal ion. The molar ratio of Ru/Sn was maintained 1:1. The Ru/Sn nominal volume ratio was 10 %. The obtained solution was stirred in an ultrasonic cleaner at room temperature for 2 hours in air to obtain intended homogeneity and turbidity. Glass substrates were cleaned in methanol for 2 hours in an ultrasonic cleaner prior to spin coating process. The solution was dropped onto glass substrates rotated at 1500 rpm for 45 s. The deposited films were then annealed at 600 °C for 1 hour in air. Coating and heating procedures were performed by three times.

X ray diffraction (XRD, Rigaku D/MAX 2200/PC) patterns of the films were determined to identify phase structure by means of a diffractometer with a CuKα irradiation. The surface properties and topographies of the films were examined using scanning electron microscopy (SEM, JEOL JSM 6060) attached with energy dispersive spectroscopy (EDS) and atomic force microscopy (AFM, Nanosurf Easy Scan) respectively. The film thickness was determined with VEECO profilometer. Shimadzu 2450

UV spectrophotometer was used for optical measurements in the wavelength range between 350 and 800 nm.

3. Results and discussion

3.1 Structural and morphological properties

XRD patterns of undoped and Ru doped SnO2 thin films deposited on Si substrates were represented in Fig. 1. Bragg peaks due to the presence of SnO2 rutile phase were observed in both of the films. In Ru doped SnO2 film, both SnO2 and RuO2 peaks were obtained. Bragg peaks for RuO2 phase were found to be at smaller intensities if compared to SnO2 peaks. This result also notes that substitution of Ru into tetragonal rutile structure was successfully applied.
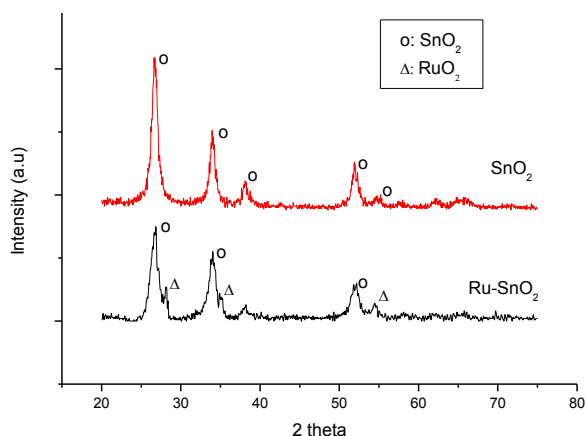
Fig. 1. XRD patterns of undoped and Ru doped SnO$_2$ nanostructure thin films on glass substrates.

Sol-gel deposition is a wet chemical route and the film quality is directly related to various parameters such as substrate interaction, pH, humidity and temperature. In order to produce crack-free and pinhole-free, oriented and homogenous films, optimization of these parameters and the control of experimental conditions are found to be very important.

SnO2 semiconducting thin films which are the one of the strong candidate for electronic sensor device must obtain all properties mentioned in the above paragraph. By this way any crack or inhomogenity on the surface could destroy the electronic structure of the films. Fig. 2 represents microstructure and morphology of the smooth and crack-free undoped and Ru doped SnO2 films. In order to support SEM results and determine surface roughness of the films, AFM analyses were applied. AFM results were depicted in Figs. 3a and 3b for undoped and Ru doped SnO2 films respectively. AFM image of the film represents nanoscale surface roughness between 1 and 20 nm. It is clear from SEM and AFM micrographs that higher part of region represent white region.
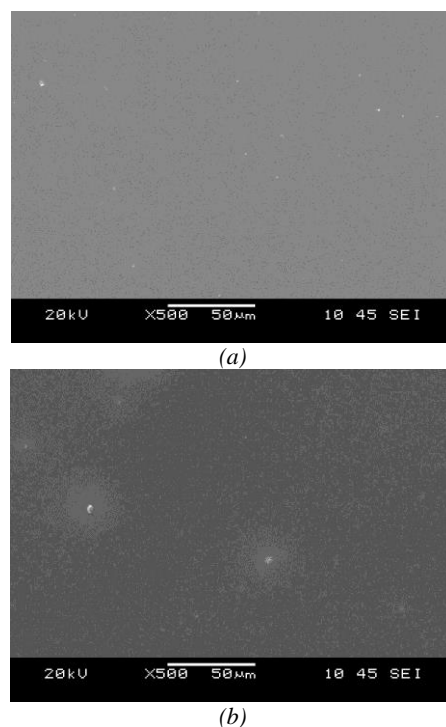
Fig. 2. SEM images of (a) undoped and (b) Ru doped SnO$_2$ nanostructure thin film.
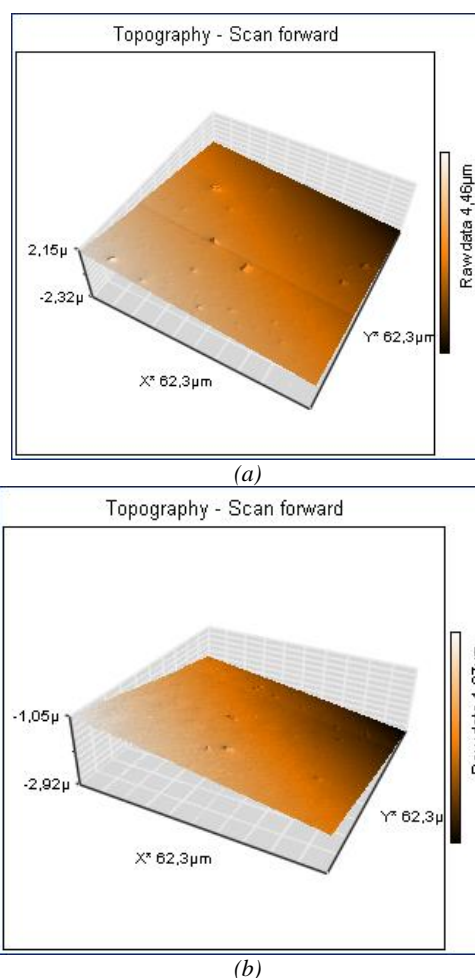
Fig. 3. AFM images of (a) undoped and (b) Ru doped SnO$_2$ nanostructure thin films.

3.2 Optical properties of the undoped and Ru doped SnO_2 films

The transmittance and reflectance spectra of the films were measured in the range of 350–800 nm, as shown in Figs. 4a and 4b, respectively. For the longer wavelengths ($\lambda > 400$ nm), all thin films become transparent and no light is scattered or absorbed as non absorbing region (i.e. $R + T = 1$). The inequality ($R + T < 1$) at shorter wavelengths ($\lambda < 400$ nm) known as absorbing region is due to the existence of absorption. The average transmission of the undoped and Ru doped SnO2 films is 97 % and 89 % for the visible region. It is seen that the transmittance is limited only by the surface reflectance between 3.7 % and 8.5 % in the visible region. This suggests that the film has a high transparency and good optical quality due to low scattering or absorption losses.

a)

b)
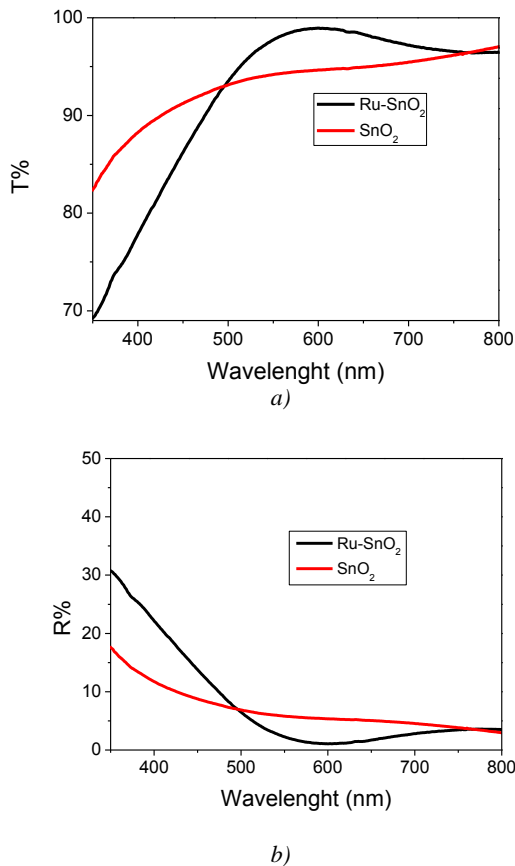
Fig. 4. (a) Optical transmittance and (b) reflectance spectra of SnO_2 and Ru-SnO_2 films.

The absorption edge also shifted slightly to higher wavelengths with addition of Ru doping. This decreasing in transmittance and reflectance may be due to incorporation of Ru as well as formation of bigger crystals and increased scattering at the grain boundaries due to the presence of Ru [16, 17].

The refractive index of the films is an important parameter for optical device design. Equation 1 can be used to calculate the refractive index at different wavelength.

$$n = \left(\frac{1+R}{1-R}\right) + \sqrt{\frac{4R}{(1-R)^2} - k^2} \qquad (1)$$

where n is the refractive index and k ($=\alpha\lambda/4\pi$) is extinction coefficient. When the thickness of film is known, then the computation can be carried out and the optical constants can be calculated. A variation of the refractive index values with respect to wavelength for undoped and Ru doped SnO_2 thin films are shown in Figure 5. The average refractive index of the Ru doped SnO_2 film is bigger than the SnO_2 film in the measured wavelength range. The rising refractive index with Ru incorporation can be attributed to the density and the surface roughness [18]. The refractive index and absorption coefficient values of undoped and Ru-SnO_2 films at 400 nm are given in Table 1. As seen from table, absorption coefficient of the SnO_2 film also increases with Ru incorporation.

Table 1. Average transmittance and reflectance values in the visible region, and optical constants of both films at $\lambda = 400$ nm.

Film	T_{ave} (%)	R_{ave} (%)	n	$\alpha \times 10^5$ (m^{-1})	E_g (eV)
SnO_2	97	3.7	2	2.1	3.76
Ru:SnO_2	89	8.5	2.75	4.3	2.98
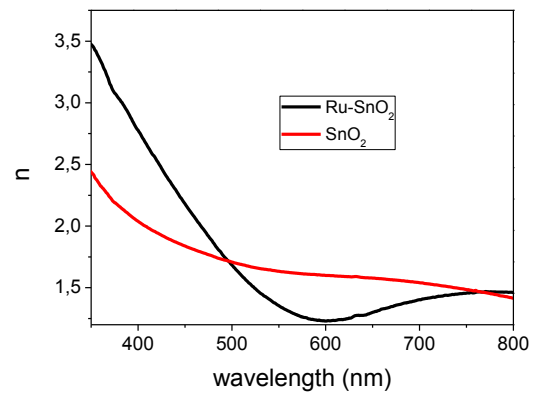
Fig. 5. The variation of refractive index of the SnO_2 and Ru-SnO_2 films.

The fundamental electron excitation spectra of the films were described by means of a frequency dependent of the complex dielectric constant. The complex dielectric constant function is expressed by the following relation,

$$\varepsilon(\omega) = \varepsilon_r(\omega) + i\varepsilon_i(\omega) \qquad (2)$$

where ε_r and ε_i are real and imaginary parts of the dielectric constant, respectively and these values were calculated using the formulas [19],

$$\varepsilon_r(\omega) = n^2(\omega) \ k^2(\omega) \quad \text{and} \quad \varepsilon_i(\omega) = 2n(\omega)k(\omega \qquad (3)$$

Figs. 8a and 8b show ε_r and ε_i values dependence of photon energy for both undoped and Ru-SnO_2 films,

respectively. The ε_r value of the SnO₂ film increases with Ru doping due to the increase in refractive index. It can be seen that the real and imaginary part of the dielectric constant values decrease with increasing wavelength in the visible region.
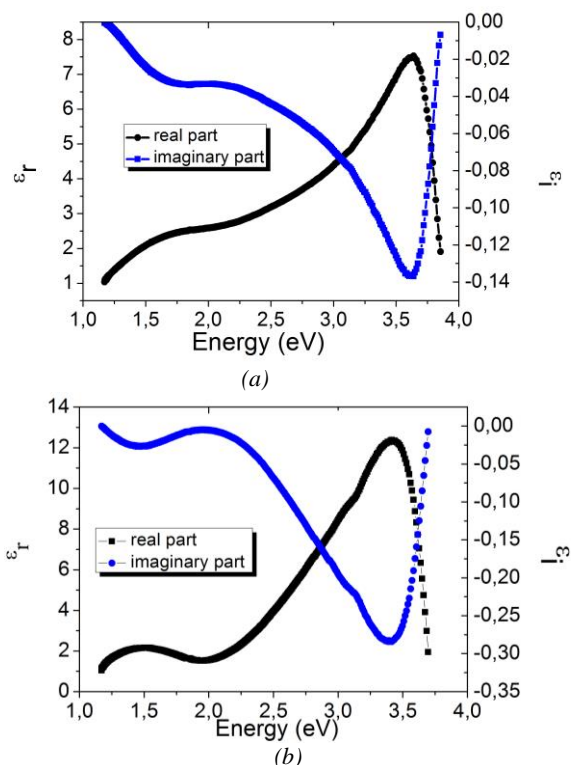
Fig. 6. The variation of real (εᵣ) and imaginary (εᵢ) parts of the dielectric constant of (a) SnO₂ and (b) Ru-SnO₂ films.

The analysis of the dependence of absorption coefficient on photon energy in the high absorption regions is carried out to obtain the detailed information about the energy band gap of the SnO₂. The optical band gap the films is determining by the following relation [20].

$$(\alpha h\upsilon) = A(h\upsilon - E_g)^m \qquad (4)$$

where A is an energy independent constant between 10^7 and 10^8 m^{-1}, m is an index that characterizes the optical absorption process and it is theoretically equal to 2 and 1/2 for indirect and direct allowed transitions and E_g is the optical band gap of the material. It is evaluated that the optical band gap of the nanostructured films has a direct optical transition [21]. It is well known that direct transitions across the band gap are feasible between the valence and the conduction band edges in k space. In this transition process, the total energy and momentum of the electron photon system must be conserved. Figs. 7a and 7b shows the plot of $(\alpha h\upsilon)^2$ vs. $h\upsilon$ of the undoped and Ru doped SnO₂ films. The optical band gap values of the films were determined from the intercept of $(\alpha h\upsilon)^2$ vs. $h\upsilon$ curves and these values were found to be 3.76 eV and 2.98 eV for undoped and Ru doped SnO₂ films, respectively. In the literature, the optical band gap of SnO₂ film was calculated in between 3.4 eV and 4.6 eV depending on

fabrication procedures and conditions [22-28]. The inconsistency in the optical band gap is due to Burstein-Moss effect reported in earlier studies [29]. According to this theory, doping causes the variation of the band gap. The band gap in this study decreased considerably for films with doping of SnO₂ with ruthenium. This decrease is attributed to the shrinkage effect of the optical band gap. Since the strong exchange interactions between d electron of Ru, and s and p electrons of SnO₂ cause the broadening of valence and conduction bands of the film, the optical band gap of SnO₂ film decreases [30]. This result is in agreement with literature with using different elements for doping and also using different fabrication methods [31-32].
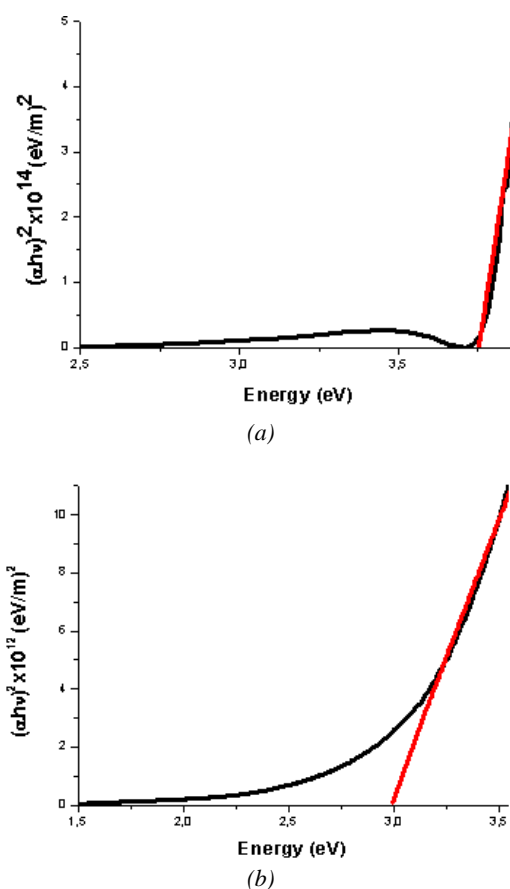
Fig. 7. Plots of (αhυ)² vs. Energy of (a) undoped SnO₂ and (b) Ru-SnO₂ films.

4. Conclusions

Undoped and Ru doped semiconducting SnO2 films were deposited on glass substrates by sol-gel technique. Structural, morphological and optical properties were significantly altered with Ru doping into SnO₂ films. XRD results revealed that all the films have tetragonal rutile and Ru incorporation affects the crystalline structure of the film. It was observed that surface was smoother with adding Ru. It was found that absorption edge shifted to higher wavelengths with incorporation of Ru, and optical band gap of SnO₂ film was decreased with the increase in Ru doping. The Ru doped semiconducting SnO₂

transparent film is very useful for solar cell applications due to high transparent of visible light and low optical band gap.

Acknowlegement

References

[1] A. Zribi, J. Fortin, Functional Thin Films and Nanostructures for Sensors: Synthesis, Physics, and Applications, Springer, Newyork, 2009.

[2] G.Shuping, X. Jing, L. Jianqiao, Z. Dongxiang, Sensors and Actuators B **134,** 57 (2008).

[3] Y. J. Choi, H. Park, S. Golledge, D. Johnson, H.J. Chang, H. Jeon, Surface & Coatings Technology **205,** 2649 (2010).

[4] L. Li, K. Yu, J. Wu, Y. Wang, Z. Zhu, Cryst. Res. Technol. **45**, 539 (2010).

[5] C. Liewhiran, N. Tamaekong, A. Wisitsoraat, S. Phanichphant, Sensors **9**, 8996 (2009).

[6] R. S. Niranjan, S.R. Sainkar, K. Vijayamohanan, I.S. Mulla, 2002, Sensors and Actuators B **82**, 82 (2002).

[7] R.D. Delgado, Tin Oxide Gas Sensors: An Electrochemical Approach, PhD. Thesis, University of Barcelona, 2002.

[8] O. Culha, M. F. Ebeoglugil, I. Birlik, E. Celik, M. Toparli, J Sol-Gel Sci Technol **51**, 32 (2009)

[9] S. M. Ali, S. T. Hussain, S. Abu Bakar, J. Muhammad, ,N. Rehman, Journal of Physics: Conference Series **439,** 012013 (2013).

[10] Y. Xiao, S. Ge, L. Xi, Y. Zhou, Appl. Surf. Sci. **254**, 7459 (2008).

[11] S.S. Roy, J. Podder Gilberto, J. Optoelectron and Adv. Mater **12**, 1479 (2010).

[12] B. Zhang, Y. Tian, J.X. Zhang, W. Cai, Appl. Physics Lett. **98,** 021906 (2011).

[13] T. Boben, B. Skariah, K.K. Radha, Sens. Actuators B **133**, 404 (2008).

[14] K. Y. Rajpure, M. N. Kusumade, M. N. Neumann-Spallart, C. H. Bhosale, Mat. Chem. And Phy. **64**, 184 (2000).

[15] E. Celik, U. Aybarc, M. F. Ebeoglugil, I. Birlik, O. Culha, J Sol-Gel Sci Technol **50**, 337 (2009)

[16] Y. S. Lee, O. S. Kwon, S. M. Lee, K. D. Song, C. H. Shim, G. H. Rue, D. D. Lee, Sensors and Actuators B: Chemical **93**, 556 (2003).

[17] S. A. Mahmoud, A. A. Akl, H. Kamal, K. Abdel Hady, Physical B **311**, 336 (2002).

[18] F. Karipcin, E. Kabalcilar, S. Ilican, Y. Caglar, M. Caglar, Spectrochim Acta A **73**, 174 (2009).

[19] J. N. Hodgson, Optical absorption and dispersion in Solids, Chapman and Hall LTD, London, 1970.

[20] M. Deepa, N. Bahadur, A.K. Srivastava, P. Chaganti, K.N. Sood, J Phys Chem Solids **70,** 291 (2009).

[21] R. Summitt, J. A. Marley, and N. F. Borrelli, J. Physics Chemistry of Solids, **25**, 1465 (1964).

[22] A. Czapla, E. Kusior and M. Bucko., Thin Solid Films **182**, 15 (1989).

[23] A.E. Rakshani, Y.H.A. Makdisi and Ramazanyan. J. Appl. Phys. **83**, 1049 (1998).

[24] P.S. Patil, R.K. Kawar, T. Seth, D.P. Amalnerkar, P.S. Chigare, Ceramics Int. **29**, 725 (2003).

[25] M. Batzill, U. Diebold, Progress in Surface Science **79**, 47 (2005).

[26] M. A. Yıldırım, S. T. Yıldırım, E. F. Sakar, A. Ates, Spectrochimica Acta Part A: Molecular and Biomolecular Spectroscopy **133**, 60 (2014).

[27] C.E. Benouis, M. Benhaliliba, Z. Mouffak, A. Avila-Garcia, A. Tiburcio-Silver , M. Ortega Lopez, R. Romano Trujillo, Y.S. Ocak, Journal of Alloys and Compounds **603,** 213 (2014).

[28] A. Benhaoua, A. Rahal, B. Benhaoua, M. Jlassi, Superlattices and Microstructures **70**, 61 (2014).

[29] C.E. Benouis, M. Benhaliliba, A. Sanchez Juarez, M.S. Aida, F. Chami, F. Yakuphanoglu, J. Alloys Comp. **490**, 62 (2010).

[30] Y. Caglar, S. Ilican, M. Caglar, F. Yakuphanoglu, J Sol-Gel Sci Technol **53,** 372 (2010).

[31] J. Joseph, V. Mathew, K. E. Abraham,Chinese Journal of Physics **45**, 84 (2007)

[32] G. Turgut, E. Sonmez, S. Aydın, R. Dilber, U. Turgut, Ceramics International **40,** 12891 (2014).

_____

*Corresponding author: omer.mermer@ege.edu.tr